FRAGMENT DRIVEN MAGNETIC RECONNECTION

K. Galsgaard[(1)] and C. Parnell[(2)]

[(1)]NBIfAFG, Astronomical Observatory, Juliane Maries vej 31, 2100 Kbh Ø, Denmark
[(2)]School of Mathematical and Statistical Sciences, University of St Andrews, St Andrews, KY16 9SS, UK

arXiv:astro-ph/0409562v1 23 Sep 2004

ABSTRACT

The heating of the million degree, diffuse coronal plasma may be caused by a large number of events that are too small to be identified by present days observations. One explanation for these events could be the local interaction between magnetic flux systems that divide space into numerous flux regions. When such regions are independently advected by photospheric motions the expected outcome is the formation of enhanced current concentration at specific locations in space. Due to magnetic resistivity, these currents dissipate and heat the plasma. In this paper, we investigate a simple model where two, initially unconnected, flux systems are forced to interact in response to the imposed boundary driving by solving the non-ideal 3D MHD equations numerically. The reconnection rate of the dynamical process is determined and compared with the corresponding rate for the potential evolution of the magnetic field. This shows that the dynamic reconnection rate is about a factor of two smaller than the potential (perfect, instantaneous) rate for realistic solar driving velocities demonstrating that this three-dimensional magnetic reconnection process is fast.

The energy input for a fixed advection distance is found to be independent of the driving velocity. The Joule dissipation associated with the reconnection process is also found to be basically dependent on the advection distance rather than driving velocity. This implies that the timescale for the event determines the effect the heating has on the temperature increase.

Finally, the numerical experiments indicate that the observational structure of the reconnection site changes dramatically depending on the phase of the evolution of the passage of the two flux sources. In the initial phase, where the sources become connected, the heating is confined to a compact region. For the disconnecting phase the energy gets distributed over a larger area due to the reconnected field line connectivity.

Key words: Sun: Corona Heating, Magnetic Reconnection.

1. INTRODUCTION

The coronal magnetic field is a manifestation of the distribution of photospheric fluxes and their continuous motion. By taking a magnetogram and representing each pixel value by a point source Close et al. (2004a) showed that each coherent flux patch connects to several neighbouring flux patches. This complex mapping of the magnetic field gives rise to many *separatrix surfaces*; shells that divide space into different regions of connectivity. In general the distance, and also the direction, of travel of the various magnetic sources differ. The movement of any one source causes the orientation of the magnetic field at the interface of the separatrix surfaces enclosing this flux region to change. It is assumed that, in general, such changes lead to these surfaces attracting current (Priest et al. 2002). If the current growth is significant magnetic reconnection is expected to occur releasing some of the free magnetic energy built up by the movement of the sources.

In the photosphere the flux sources are continuously moved around by the convective motions and stresses like those indicated above must be taking place at many locations above the photosphere. From detailed analysis of magnetograms, Hagenaar et al. (2003) showed that the recycle time of the photospheric flux is on the order of 8-19 hours. During this time flux sources emerge into the photosphere, where after they undergo merging, fragmentation and annihilation resulting in the loss of their identity. Flux sources are also advected resulting in a complex magnetic field. A direct consequence of all this activity is that the connectivity of the sources must change on a timescale that is much shorter than the turn over time of the sources themselves (Close et al. 2004b). These processes all contribute locally to the heating of the coronal plasma, but their individual contributions may not be as prominent and easily observed as large flares. In the past, numerous models have been investigated for coronal heating. Most of these concern processes where flux emergence or annihilation releases the energy (e.g., Uchida & Sakurai, 1977; Forbes & Priest, 1984; Shibata, Nozawa & Matsumoto, 1992; Dreher, Birk & Neukirch, 1997; Yokoyama & Shibata, 2001; Zhang & Low, 2002; Priest, Parnell & Martin, 1994; Parnell, Priest & Titov, 1994; Birk, Dreher & Neukirch, 1996). In contrast, the situation where the flux is not emerged or annihilated, but instead is forced to interact with flux from a different source, have not been investigated in great detail. This process, which is highly likely to take place in the solar magnetic field, was first investigated using the minimum current approach (Longcope 1998), where the interaction between independent flux sources in a constant background magnetic field is investigated. This work showed that as the flux systems start to interact the free energy in the field accumulates, in the form of a current sheet, at the separator line connecting two null points in the photospheric plane. Similarly, the same is found when the sources start to disconnect again. This scenario of independent flux systems first connecting and then disconnecting was investigated using numerical experiments (Galsgaard et al. 2000). They showed that the initial pro-

cess through which the two flux sources connect follows the same pattern, namely that the two sources connect through separator reconnection. In the disconnection phase, however, the reconnection occurs through a different process - separatrix-surface reconnection. This stage of the evolution is clearly different from the minimum current approach.

In this paper, we discuss the results of a series of numerical experiments that are conducted to investigate these basic processes of the flux interaction in more detail. In particular, the analysis concentrates on the reconnection process, determining a scaling relation between the numerical reconnection rate and the comparable rate for the potential evolution of the field structure, i.e., the perfect, instantaneous reconnection rate. Further, an analysis of the global energy input/output is investigated. Finally, a simple analysis of the magnetic structure of the newly reconnected field lines has been made, visualising the regions that would be exposed to large temperature increases as a result of the on going magnetic reconnection.

2. MODEL SETUP

The intention with the experiment is to investigate the simplest possible situation where two independent flux sources interact without loss (or gain) of flux from the sources. This is obtained by setting up a situation where two, oppositely-signed, flux sources are located a short distance apart on the bottom boundary of a Cartesian domain. To remove the dipole structure the two sources would generate if on their own, a constant horizontal magnetic field is added. By changing the orientation of this overlying field component the field from the independent flux domains can be changed from running parallel passed the other source, to parallel away from the other source. Introducing an advection velocity on the sources adds a preferred direction to the setup. The advection velocity is applied such that the flux domains of the two sources are forced to interact with each other. As they interact strong current concentrations are generated and eventually drive magnetic reconnection as the sources are advected passed one another. In Fig. 1 the situation adopted in Galsgaard et al. (2000) is shown. Here, the isosurfaces show the locations of the magnetic flux concentrations. The field lines starting close to the bottom boundary indicate the separatrix surfaces dividing the space into three magnetically independent flux regions. In comparison, the large scale magnetic field is indicated by the field lines close to the top boundary of the domain. On the bottom boundary, the vectors show the structure of the imposed velocity. Notice, that the driving profile is such that it maintains the structure of the sources.

The dynamical evolution of the system is investigated by solving the non-ideal 3D MHD equations numerically using the code described by Nordlund & Galsgaard 1995.

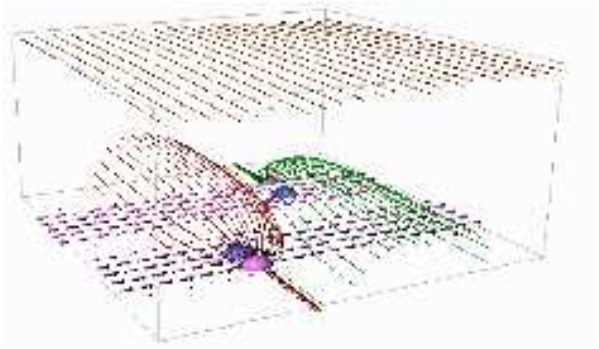

Figure 1. An example of the initial conditions used in the experiments. The blue isosurfaces show the locations of the magnetic sources. The pink isosurfaces shows the location of two magnetic null points. The brownish field lines close to the top boundary shows the large scale magnetic field structure. The two other sets of field lines, red and green, indicate the location of the separatrix surfaces dividing space into independent flux regions. The arrows at the bottom boundary indicate the profile and direction of the imposed driving velocity.

3. INTERACTION OF THE FLUX DOMAINS

Experiments have been conducted with a number of different orientations of the overlying magnetic field. The implications of this are, first, the distance the sources have to be advected before the two flux domains start to interact vary with the overlying field angle; and second, so does the velocity perpendicular to the field in the flux domains. At all orientations of the overlying field, the same general evolution takes place. As the two flux domain are forces into each other a separator current sheet is formed connecting the two null points located on the bottom boundary. As the current magnitude reaches the numerical limit magnetic *separator* reconnection starts and new field lines are created connecting the two sources. This process continues until the two sources are well passed their point of closest approach and the two sources are well connected. Eventually current concentrations start forming over the separatrix surface that encloses the connected flux resulting in *separatrix-surface* reconnection that disconnects this field. The two evolutionary phases are shown in Fig. 2, where the large isosurfaces represent the locations of the current sheets responsible for the reconnection and the field lines indicate the local and global connectivity of the magnetic field.

4. MAGNETIC RECONNECTION RATES

An important factor of magnetic reconnection in three-dimensions relates to the speed at which the process can take place. From two-dimensional magnetic reconnection (see Priest & Forbes 2000 and references there in) it is know that the speed of magnetic reconnection depends critically on the boundary conditions of the investigated domain. Furthermore, most of the previous works have concentrated on steady-state situations. Here, the situation is different, the system is driven and it reacts to the

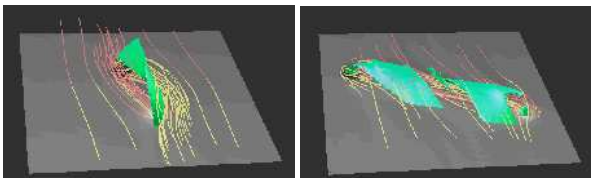

Figure 2. Left, the situation where separator reconnection dominates the dynamical evolution. Right, the situation at a later time where the field has started to disconnect through separatrix-surface reconnection. The green isosurfaces indicate the locations of strong current, while the field lines indicate the structure of the magnetic field.

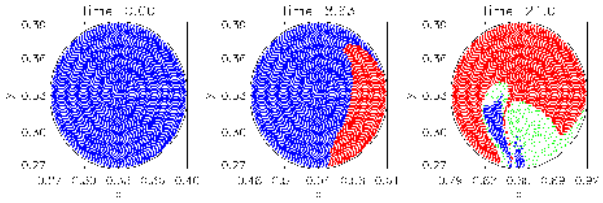

Figure 3. The field line connectivity at three different times. The colour coding represents different types of field line connectivity: blue indicates initially unconnected flux, red represents connected flux and green represents the disconnected flux.

stresses created by the boundary motions and therefore finds it's own "boundary conditions" in the language of Priest & Forbes (1986) and in this sense finds its own steady state.

To investigate the rate of change in connectivity a large number of field lines have been traced from the foot points of each source, (Parnell & Galsgaard 2004). As the source structure is maintained in time, each field line can simply be associated with a fixed amount of flux. Therefore as the field lines change connectivity the amount of flux involved in each process can be counted. In Fig. 3, three snapshots showing the structure of the field line connectivity are shown. In these snapshots, blue represents the initially unconnected flux, red indicates the field lines that connect the two sources and the green area is associated with field lines that have been disconnected. These graphs show that the change in connectivity takes place in a non-trivial manner, providing a complex mapping of the field line connectivity. In the potential extrapolation of the coronal magnetic field by Close et al (2004a), it was shown that the field line mapping of individual sources can connect to several neighbouring sources at the same time. From the mapping diagrams shown in Fig. 3 it is seen that, even for this simple case, the connectivity map contains three different types of field line connectivity. This suggests that the mappings of Close at al (2004a) provide only a lower limit in terms of complexity and that the added effects of the dynamical evolution may increase the complexity of the field line connectivity of the coronal field even further.

Another important effect of the dynamical evolution is

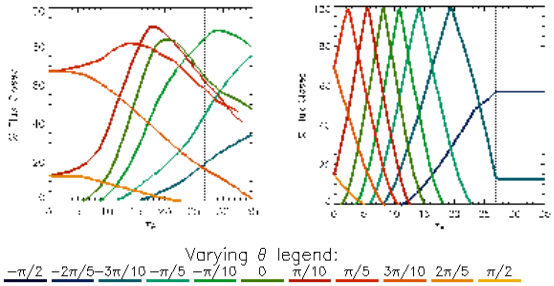

Figure 4. Left, the change in connected flux as a function of time for the experiments with different angles of the overlying horizontal magnetic field. Right, the comparable graphs for the potential evolution of the experiments.

the fact that multiple reconnection events take place at different spatial locations. This is clearly seen from the graphs showing the change in connectivity as a function of time where it is found that the reconnection processes connecting and disconnecting the flux systems, for a limited time interval, take place simultaneous. In Fig. 4 an example of the time depended evolution of the connected flux is shown. The left panel shows the evolution in the situation where the magnetic field is assumed to always relax down to a potential magnetic field configuration. In the right panel, the comparable evolution is shown for the dynamical MHD development of the system. Since both connecting and disconnecting take place at the same time, to derive a simple reconnection rate for the system both processes must be taken into account. The process of tracking the field line connectivity provides a possibility for doing exactly this. The amount of flux belonging to any of the three classes are therefore easily obtained as a function of time. Taking the time derivative of these and normalising the result with regard to the characteristic Alfvén velocity of the domain and the total flux in a source, gives a dimensionless measure of the reconnection speed.

From Fig. 4 it is seen that the fraction of connected flux between the two sources depends both on the angle of the overlying magnetic field and the driving speed and clearly on whether the evolution is potential or the dynamical MHD solution. The time derivative of these curves gives a measure of the rate of change of the connectivity, which is equivalent to measuring a connecting reconnection rate. Similar graphs can be obtained for the disconnecting process and hence the disconnecting reconnection rate. By comparing these phases it is found that the connecting and disconnecting of the field in the potential case occurs at the same rate. In the dynamical experiment, however, these processes are found to evolve at two different rates; with the peak connecting rate found to be about twice that of the peak disconnecting rate. This difference in reconnection rates is a consequence of the apparent stress of the magnetic field for the two process. In the connecting process the two independent flux systems are forced into each other as the system responds to the advection of the sources and the only way to release this stress is to generate a local

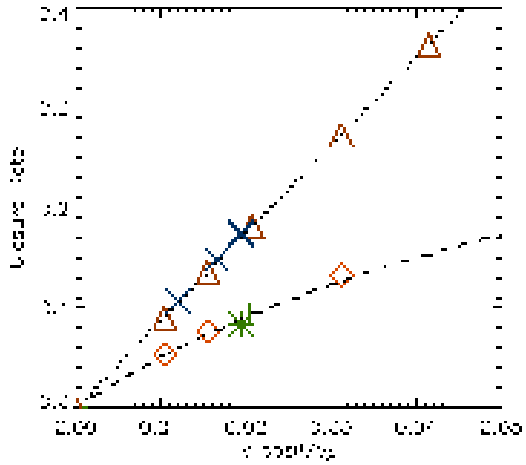

Figure 5. The peak total reconnection rate for the potential evolution (dotted line) and the dynamical evolution (dashed line). The symbols represent the various individual experiments while the lines are lines of best fit given by Eq. (2) and Eq. (1), respectively.

current sheet through which magnetic reconnection can take place. In the following disconnecting process, reconnection takes place between open overlying magnetic field and the connected field which is advected under this. Here, the stresses between the two flux regions are less, as the overlying open field can simply be lifted up over the connected (dipole) field. The developing separatrix current sheets are consequences of the increasing tangential change in the field line orientation between these two flux systems and the pushing of them together by the magnetic tension and magnetic pressure forces in the two systems.

Adding the rates of connecting and disconnecting gives the total reconnection rate at any one time. The result of this is seen in Fig. 5, which shows both the potential (perfect, instantaneous) reconnection rate and the comparable result for the dynamical evolution for all the conducted experiments. This graph doesn't provide detailed insight to the reconnection process, but shows how that the accumulated peak reconnection rate for the experiments depend, in a systematic way, on the driving velocity perpendicular to the direction of the overlying magnetic field. In Fig. 5, the dotted line represents the potential evolution of the magnetic field, while the dashed line represents the dynamical evolution. The important information contained in this diagram can be condensed to the following expressions for the two reconnection rates:

$$R_{pot} = 8.8 v_d \cos\theta, \quad (1)$$

$$R_{dyn} = \frac{0.6 v_d \cos\theta}{v_d \cos\theta + 0.11}, \quad (2)$$

where $v_d \cos\theta$ is the driving velocity perpendicular to the direction of the overlying magnetic field, which also represents the direction perpendicular to the developing current sheet. This shows that for slow driving velocities the dynamic peak reconnection rate approaches the potential rate, while for increasing driving velocities it approaches a constant rate whereas the potential rate continues to grow linearly. For realistic driving velocities in the solar context, this indicates that the magnetic reconnection rate, here, is fast, at just a factor of two less than the potential rate.

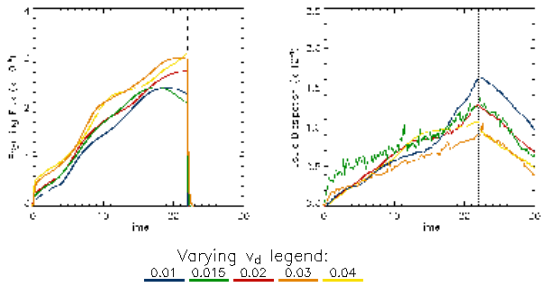

Figure 6. Left, the pointing flux for five experiments with different driving velocity. The graphs are scaled according to Eq. (3) to give the same absolute value as a function of advection distance. Right, the average Joule dissipation. As a first approximation, the energy released from all the experiments, over a given advection distance of the sources, may be considered the roughly same. The colours of the lines represent different driving velocities.

5. ENERGY CONSIDERATIONS

Taking the result from the previous section, namely that the reconnection is fast and within a factor of two of that the required for the field to maintain a potential state, one may assume that the energetics of the system could simply be represented using a potential model (Galsgaard & Parnell 2004).

If the driving velocity is slow and has a duration that is long compared to the Alfvén crossing time then the Poynting flux input can be estimated by,

$$P_f \approx \mu \frac{B_n v_d^2 t_d}{L}, \quad (3)$$

where B_n is the normal component of the magnetic field, v_d is the driving velocity, t_d is the duration of the driving and L is the distance to the anchored (fixed) end of the field line. This reveals that the energy input scales quadratically with driving speed and linearly with duration. Integrating Eq. (3) over a fixed advection distance suggests that the same amount of energy should be injected to the magnetic configuration independent of the driving velocity. These results have been tested by conducting a series of experiments with different driving velocities. Scaling the amplitudes of the Poynting flux to the advection distance indicates that the results follow the simple scalings obtainable from Eq. (3) to within a velocity dependent initial offset, left panel of Fig. 6. The initial difference is due to the change in ratio between the driving velocity and the local Alfvén velocity and holds as long as the information can propagate freely away from

the driving boundary. It is only when the initial perturbation of the field lines, which is generated when the driving is first switched on, reaches another anchor point of the field line that the effect of the angle of the field (caused by the driving) start to be felt leading to a linear increase in time of the Poynting flux according to Eq. (3).

If the same amount of energy is injected into the domain for a given advection distance regardless of driving speed, then in each case the same amount of energy is available for heating the plasma through dissipation. The dynamical evolution of the various cases follow similar patterns and so it is not unreasonable to expect the energy release to be of comparable magnitude. The Joule dissipation for the numerical domain is plotted as a function of advection distance and scaled to the same driving time in right panel of Fig. 6. This panel shows that only minor differences in the energy release exist between the different cases over the same advection distance, and that most of these can be accounted for by the differences in the ratio between the Alfvén crossing time and the driving time for a given advection distance. The effect of the energy release, on the other hand, depends linearly on the timescale over which it is released. The shorter the timescale the greater the impact of the energy release.

The amount of Poynting flux and Joule dissipation cannot be estimated using potential models, as they depend critically on the magnetic fields reaction to the imposed driving, and through this on the change in angle of the local magnetic field lines stressed by the boundary driving. This angle is a result of a balanced between the geometry of the magnetic field, the local current concentrations and the efficiency of the magnetic resistivity.

6. PLASMA STRUCTURE OF THE ENERGY RELEASE

The models used in these investigations have been setup to investigate the effects of magnetic reconnection in a simple magnetic structure. But they can also be used to attempt to investigate the change in the visual appearance of heated magnetic structures as the type of reconnection changes with time. The best and only realistic way to do this is to include: i) a more detailed model atmosphere; ii) the effects of optically thin radiation and anisotropic heat conduction in the energy equation. The disadvantage with this is the requirement for background heating to balance the radiation and conduction in the initial configuration which one cannot easily justify in the given system. Instead, a more simplistic approach to illustrate the effect has been adopted here. From the field line tracing mentioned above it is straight forward to identify the starting points of the field lines that change connectivity between the snapshots. A realistic assumption to then make is that the energy released in the reconnection event scales with the magnetic flux represented by the field line. Distributing this energy evenly along the field lines, a local temperature increase of the plasma may then be estimated with the inclusion of a vertical density profile along the field lines. Here, the plasma density is assumed to decreases rapidly with height following a simple hyperbolic tan function. This simple model emulates a photosphere at the driving boundary follow by a shallow transition region, while most of the domain contains a coronal plasma density. Then by following the reconnected field lines, local temperature increases can be calculated which, when all contributions are summed, reveal a few interesting conclusions as the system evolves in time (Fig. 7).

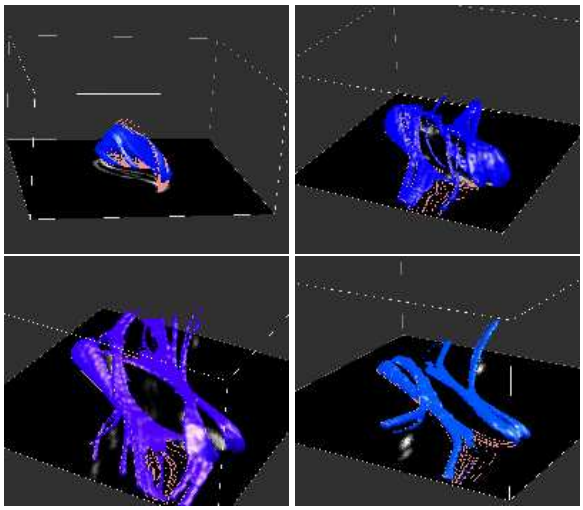

Figure 7. The four panels show the structure of the heated plasma at different times during the evolution of the flux systems in one experiment. Only the regions with temperatures above the initial coronal temperature are shown.

- The initial connecting of the magnetic field between the two sources gives rise to a compact structure outlined by field lines that link the two sources.
  - Note, that a limitation here is the problem with identifying the newly reconnected open field lines which are not identified. These coronal field lines may, however, be so long that the energy distributed along them from the reconnection has only limited impact on rising their temperature.
- When the field starts to disconnect the field lines extend from the sources to the open coronal field again and the energy is distributed along field lines that might reach far away from the reconnection site.
- Furthermore, the disconnecting process is not equally active all across the whole separatrix surface, but is more stochastic in nature leading to several fingers of field lines leading away from the sources.

Taking the simplicity of the approach into account it is clear that to fully see the thermal, and therefore observational appearance of the reconnecting structure, the problem has to be solved consistently including the effects of optical thin radiation and anisotropic heat conduction. An

interesting, but difficult task to handle consistently and clearly a problem for future investigations.

7. SUMMARY

The numerical experiments discussed in this paper investigate a simple situation where two initially unconnected flux sources are forces into each other by an imposed velocity profile on the photospheric boundary. From the experiments the following main conclusions arises:

- The reconnection initially leading to the connection of the two sources occurs in the form of separator reconnection along the degenerate separator line connecting two magnetic nulls located in the photospheric plane.
- The disconnecting of this flux takes place through separatrix-surface reconnection.
- Mapping the changes in connectivity of one source, as a function of time, shows a complicated connectivity map with a clear overlap between initially unconnected, connected and disconnected flux.
- Reconnection speeds for the two process have been obtained showing that separator reconnection connecting the field is about twice as fast as the separatrix-surface reconnection that disconnects the field.
- The dynamical model is found to be about a factor of two slower, for realistically slow driving velocities, than a potential model in which instantaneous perfect reconnection occurs. In other words, *the reconnection is fast*!
- The Poynting flux injected through the imposed driving depends mainly on the advection distance and only to a small degree on the driving velocity. This result cannot be obtained using potential models.
- Similarly, the time integrated Joule dissipation between the various experiments is comparable for a given advection distance. This implies that the effect of the energy deposition depends critically on the timescale of the energy release.
- The reconnected magnetic field lines form a compact structure linking the two flux sources, giving rise to a very local area of plasma above the background coronal temperature.
- In the disconnecting phase the reconnected (heated) field lines create a complicated web of hot filaments extending into the corona.

In terms of observational appearance of the flux interaction the applied model is very simple and more detailed investigations, including a more realistic treatment of the energy equation are required. This is work that has to be done, if we want to conduct detailed comparisons between numerical models and observations.

ACKNOWLEDGMENTS

KG would like to thank PPARC and Carlsberg for financial support over various periods of this work in the from of two fellowships. CEP would like to thank PPARC for support as an Advanced Fellow. The computational analysis for this paper was carried out on the joint SRIF and PPARC funded linux cluster, copson, in St. Andrews.

REFERENCES

Birk, G., Dreher, J. & Neukirch, T. 1996, A.S.P. Conf. Ser. Vol 111, Magnetic Reconnection in the Solar Atmosphere, eds. R.D. Bentley and J.T. Mariska, 89

Close, R., Parnell, C., Longcope, D. Priest, E. R., 2004, ApJL, 612, L81

Close, R., Parnell, C., Mackay, D. H. Priest, E. R., 2004, Solar Physics, 212, 251

Dreher, J., Birk, G. & Neukirch, T. 1997, Astronomy & Astrophysics, 323, 59

Forbes, T. G. & Priest, E. R. 1984, Solar Physics, 94, 315

Galsgaard, K., Parnell, C. & Blaizot, J., 2000 A&A, 362, 383

Galsgaard, K. & Parnell, C., 2004, work in progress

Hagenaar, H. J., Schrijver, C. J. & Title, A. M., 2003, ApJ, 584, 1107

Longcope, D. 1998, ApJ, 507, 650

Nordlund, Å. & Galsgaard, K. 1995, A 3D MHD code for Parallel Computers, Technical Report, Astronomical Observatory, Copenhagen University.

Parnell, C. E., Priest, E. R. & Titov, V. S. 1994, Solar Physics, 153, 217

Parnell, C. & Galsgaard, K., A&A, 2004, inpress

Priest, E. R., Heyvaerts, J. & Title, A. M., 2002, ApJ, 576, 533

Priest, E. R. & Forbes, T. G., 1986, JGR, 91, 5579

Priest, E. R. & Forbes, T. G., 2000, Magnetic Reconnection: MHD Theory and Aplictions, Cambridge University Press

Priest, E. R., Parnell, C. E. & Martin, S. F. 1994, ApJ, 427, 459

Shibata, K., Nozawa, S. & Matsumoto, R. 1992, PASJ, 44, 265

Uchida, Y. & Sakuri, T. 1977, Solar Physics, 51, 413

Yokoyama, T. & Shibata, K. 2001, ApJ, 549, 1160

Zhang, M. & Low, B. C. 2002, ApJ, 576, 1005